GEOPHYSICAL RESEARCH LETTERS, VOL. 40, 5295–5299, doi:10.1002/grl.50970, 2013

Structural evolution of monsoon clouds in the Indian CTCZ

Kamalika Sengupta,[1] Sagnik Dey,[1] and Mampi Sarkar[1]

Received 16 August 2013; accepted 17 September 2013; published 4 October 2013.

[1] Structural evolution of monsoon clouds in the core monsoon region of India has been examined using multisensor data. Invigoration of warm clouds above 4.5 km (occurring in only 15.4% days of the last 11 monsoon seasons) is associated with a transition from negative to positive normalized rainfall anomaly. Cloud top pressure reduces with an increase in aerosol optical depth at a higher rate of invigoration in drier condition (characterized by large fraction of absorbing aerosols) than wet condition. Cloud effective radius for warm clouds does not show any significant change with an increase in aerosol concentration in the presence of high liquid water path, probably due to strong buffering role of meteorology. The structural evolution of monsoon clouds is influenced by both dynamic and microphysical processes that prolong the cloud lifetime, resulting in infrequent rainfall. Our results call for improved representation of aerosol and cloud vertical structures in the climate models to resolve this issue. **Citation:** Sengupta, K., S. Dey, and M. Sarkar (2013), Structural evolution of monsoon clouds in the Indian CTCZ, *Geophys. Res. Lett.*, *40*, 5295–5299, doi:10.1002/grl.50970.

1. Introduction

[2] Aerosol-cloud-precipitation interplay is a highly debated topic [*Tao et al.*, 2012; *Andreae and Rosenfeld*, 2008], particularly in the Indian monsoon region characterized by large aerosol loading [*Ramanathan et al.*, 2005; *Lau and Kim*, 2006; *Bollasina et al.*, 2011; *Ganguly et al.*, 2012]. Lack of robust in situ observations of coincident aerosol and cloud microphysical properties and discrepancy in satellite measurements of these properties [e.g., *Kahn et al.*, 2009; *Stubenrauch et al.*, 2013] make it difficult to evaluate the treatment of aerosol-cloud interaction and further address this issue. Very few studies exist in the literature focusing on the variability of cloud properties in the Indian monsoon region based on observations. The Indian Ocean Experiment was the first coordinated effort to measure collocated aerosol and cloud microphysical properties over the Indian Ocean providing evidence for indirect [*Heymsfield and McFarquhar*, 2001] and semidirect [*Ackerman et al.*, 2000] effect. The Continental Tropical Convergence Zone (CTCZ) campaign provided first opportunity to investigate the problem over the land region [*Jaidevi et al.*, 2011]. Subsequently, CAIPEEX campaign carried out detailed airborne measurements over the Indian CTCZ region in the monsoon season [e.g., *Konwar et al.*, 2012; *Pandithurai et al.*, 2012] to improve the parameterization of cloud microphysical processes.

[3] While these recent campaigns were successful in providing some insight into the aerosol-cloud interaction, several issues remain unresolved. For example, the structural evolution of monsoon clouds (i.e., changes in the cloud vertical structure) as the monsoon season progresses is not well understood. Moreover, the cloud properties (both macrophysical and microphysical) are sensitive to aerosols via microphysical as well as dynamical/radiative feedback [*Koren et al.*, 2008; *Li et al.*, 2011]. Precipitation data suggest that the Indian CTCZ region experienced eight normal monsoon and three deficit monsoon seasons (years 2002, 2004, and 2009) in the last 11 years. Whether the observed interannual variability in precipitation is reflected in the structural evolution of monsoon clouds needs to be examined. In this paper, we present the analysis of multisensor satellite data to study the variation of cloud vertical structure and effective radius of cloud droplets (R_{eff}) as a function of precipitation to examine the possible role of aerosols on the modulating cloud properties (and hence on precipitation). The analysis was carried out in the core monsoon region (defined by 20°N–25°N and 70°E–88°E), where the variation of rainfall shows a significant correlation (0.87) to the all-India rainfall [*Gadgil*, 2003].

2. Satellite Data and Methodology

[4] We analyze Multiangle Imaging SpectroRadiometer (MISR)-derived cloud fraction by altitude (CFbA) daily product for the cloud vertical structure for the period of 11 monsoon seasons (June–September) during the period 2000–2010. MISR detects cloud tops using a stereo technique and the relative frequency of cloud top height (CTH) between the surface and 20 km altitude at each 500 m vertical resolution within 1° × 1° grid is processed as daily level 3 CFbA product [*Marchand et al.*, 2010]. The technique is less sensitive to radiometric calibration error, but fails to detect thin cirrus clouds with optical depth less than 0.3 [*Prasad and Davies*, 2012]. Detailed discussion about the quality of this product and intercomparison with active remote sensing-based cloud vertical structure are available in the literature [*Marchand et al.*, 2010; *Wu et al.*, 2009]. In brief, MISR captures the vertical structure of low, medium, and optically thick high level clouds reasonably well compared to the active remote sensing, but under-estimates thin cirrus clouds due to the limitation in stereo technique. Active remote sensing data are available (e.g., CALIPSO and CloudSat) for the present analysis, but their shorter temporal coverage (July 2006 onward) and narrower swath relative to MISR lead to low sampling frequency for robust analysis using daily data.

Additional supporting information may be found in the online version of this article.

[1]Centre for Atmospheric Sciences, Indian Institute of Technology Delhi, New Delhi, India.

Corresponding author: S. Dey, Centre for Atmospheric Sciences, Indian Institute of Technology Delhi, Hauz Khas, New Delhi 110016, India. (sagnik@cas.iitd.ac.in)

0094-8276/13/10.1002/grl.50970

Table 1. Mean ($\pm 1\sigma$) Values of Aerosol and Cloud Parameters for the Five Ranges of Normalized Rainfall Anomaly (R) in the Core Monsoon Region During the Monsoon Season (June–September) for the Period 2000–2010

	$-2 < R < -1$	$-1 < R < 0$	$0 < R < 1$	$1 < R < 2$	$R > 2$
# Days (% of days)	185 (13.8)	596 (44.4)	354 (26.4)	147 (10.9)	60 (4.5)
AOD	0.469 ± 0.21	0.448 ± 0.19	0.481 ± 0.24	0.420 ± 0.23	0.453 ± 0.18
AI	1.21 ± 0.6	1.05 ± 0.5	0.99 ± 0.4	0.90 ± 0.3	0.83 ± 0.26
f_c	0.619 ± 0.02	0.661 ± 0.01	0.608 ± 0.01	0.548 ± 0.02	0.486 ± 0.02
cf_l	0.324 ± 0.03	0.278 ± 0.04	0.206 ± 0.04	0.312 ± 0.05	0.329 ± 0.07
cf_m	0.121 ± 0.02	0.139 ± 0.01	0.109 ± 0.01	0.116 ± 0.02	0.087 ± 0.02
cf_h	0.175 ± 0.01	0.244 ± 0.01	0.293 ± 0.02	0.119 ± 0.01	0.070 ± 0.01
$R_{eff,l}$ (μm)	14.3 ± 2.1	15.1 ± 2.0	15.9 ± 1.7	16.2 ± 1.3	16.7 ± 1.0
$R_{eff,m}$ (μm)	15.5 ± 2.8	16.7 ± 2.6	18.0 ± 2.2	18.6 ± 1.8	19.4 ± 1.3
$R_{eff,i}$ (μm)	23.3 ± 5.4	22.7 ± 3.5	22.8 ± 2.5	23.1 ± 2.2	22.9 ± 1.5
CTP (hPa)	641.3 ± 181	549.9 ± 163	447.2 ± 132	421.8 ± 115	359.9 ± 82

[5] Cloud microphysical parameters (liquid water path, *LWP* and R_{eff}), cloud top pressure (CTP), and columnar aerosol optical depth (at 550 nm), *AOD*, are taken from Moderate Resolution Imaging Spectroradiometer (MODIS) onboard the same Terra satellite (on which MISR is also flying). Level 3 (spatial resolution of $1° \times 1°$) daily C005 data for the same period were analyzed. Global validation of MODIS *AOD* was discussed in *Levy et al*. [2010], while *LWP* and R_{eff} were found to be highly correlated with in situ data, but with a high bias [*Min et al*., 2012]. Aerosol Index (AI) data were taken from Ozone Monitoring Instrument to characterize absorbing aerosols. Typically, $\mathrm{AI} > 0.2$ denotes absorbing aerosols [*Torres et al*., 2007].

[6] Anomaly in cloud vertical structure within the core monsoon region was derived with respect to mean seasonal cloud vertical structure for the 11 monsoon seasons based on 1342 daily observations and normalized with respect to 1σ. This is carried out to minimize error in MISR retrieval of cloud vertical structure when no ground truth data are available to truly evaluate the accuracy of the product. Total cloud fraction (f_c) is obtained by summing up the cloud fractions at all altitude bins, while cloud cover of low (CTH ≤3 km), midlevel (3 km < CTH ≤ 6 km), and high (CTH > 6 km) clouds is also estimated and further partitioned into low (cf_l), midlevel (cf_m), and high clouds (cf_h) to understand the overall variation of cloud vertical structure within the core monsoon region.

[7] We also used Tropical Rainfall Measuring Mission (TRMM) TMI data for the daily precipitation in each $1° \times 1°$ grid within the core monsoon region. The rainfall anomaly normalized with respect to the standard deviation (R) is estimated based on the daily rainfall data of 11 monsoon seasons. Of the total 1342 days in the last 11 monsoon seasons, 58.2% show negative R, while large precipitation events ($R > 2$) occurred in only 4.5% of the days (Table 1). All aerosol and cloud parameters are classified for five regimes of R, $-2 < R < -1$, $-1 < R < 0$, $0 < R < 1$, $1 < R < 2$ and $R > 2$ in the present work.

3. Results

[8] Figure 1 shows the variations of f_c, cf_l, cf_m, and cf_h in response to an increasing *AOD* (at 0.05 bins) within the core monsoon region. f_c increases with an increase in *AOD* at a rate (statistically significant at 99% confidence interval, CI following *t*-test, p value < 0.01) of 0.4 per unit increase in *AOD*. At very low *AOD* (<0.2), f_c is mostly contributed by high clouds, which are diagnosed as cirrus based on MISR-CTH and MODIS-CTP and cloud optical depth data. As *AOD* increases, low clouds tend to form (as indicated by large increase in cf_l) and continues to dominate (~70% contribution to f_c) until *AOD* reaches 0.3. We note that the low-level cloudiness continues to increase even with an increase in *AOD* beyond $AOD > 0.3$. However, the relative proportion of low clouds reduces at $AOD > 0.3$ because of formation of midlevel and high clouds, as shown by statistically significant (at 99% CI) increase of cf_m and cf_h for rise of f_c at higher *AOD* (Figure 1). The observed relationship between f_c and R reveals that mean f_c initially increases with an increase in R followed by a decrease when R becomes positive (Table 1). The initial increase in f_c at negative R may well be attributed to development of midlevel and high clouds in the presence of large *AOD*. Subsequently, cf_h reduces when R exceeds 1, implying that most of the precipitation occurred when f_c is dominated by high clouds. As cf_h increases, cf_l reduces with an increase in R until R exceeds 1 beyond which it again increases (Table 1). This suggests a transition from low to high cloud regime for initiation of

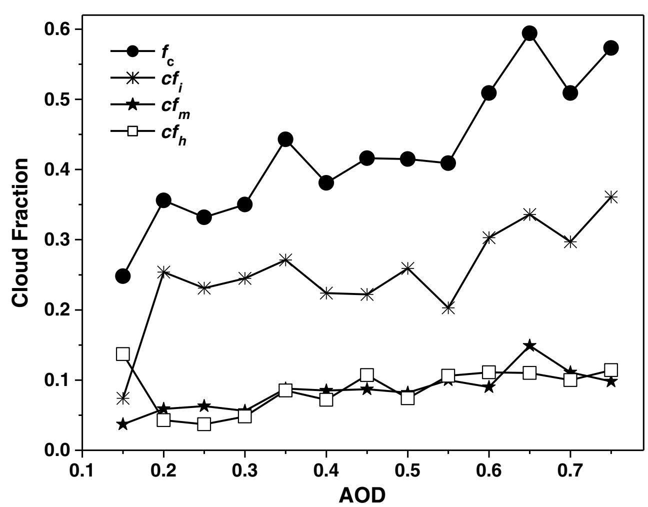

Figure 1. Variations of total cloud cover (*fc*), low cloud cover (*cfl*), midlevel cloud cover (*cfm*), and high cloud cover (*cfh*) with an increase in *AOD* within the core monsoon region. The values in the *x* axis represent the lower range of the *AOD* bins with the last bin showing statistics for $AOD > 0.7$. Statistics are generated for the 11 monsoon seasons (June–September) in the period 2000–2010.

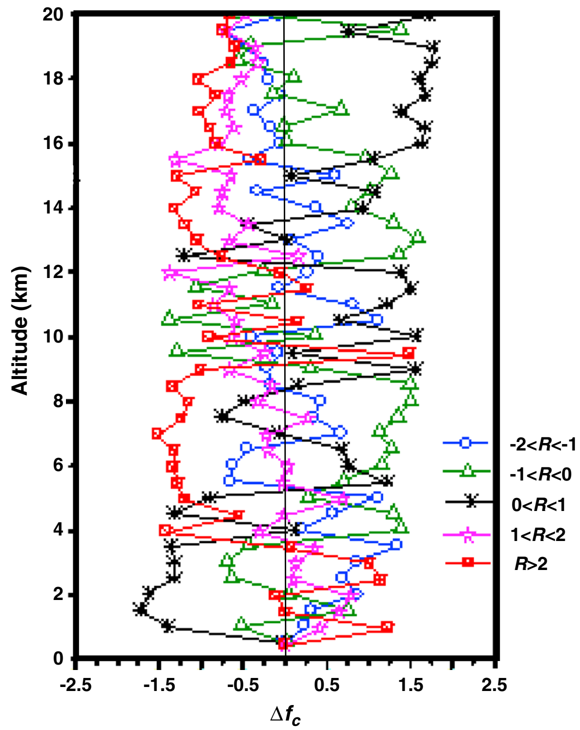

Figure 2. Vertical profiles of normalized *fc* anomaly (Δfc) derived from MISR within the core monsoon region at various ranges of normalized rainfall anomaly (R).

precipitation. However, when it does, low clouds continue to build up in the presence of persistent aerosol concentrations and enough moisture (as indicated by *AOD* values in Table 1).

[9] It is tempting to attribute the observed *AOD*-f_c relation to aerosol indirect effect. For example, persistence of large aerosol concentration throughout the monsoon season may have enhanced cloud lifetime and therefore f_c increases with an increase in *AOD*. However, the *AOD*-f_c relation (even *AOD*-cf_l relation) does not correspond to microphysics-radiation effect reported in literature [*Koren et al*., 2008; *Small et al*., 2011]. We attribute this difference to meteorology. Large-scale convection (relative to the winter season, when microphysics-radiation effect in *AOD*-cf_l relation was observed over the Indian Ocean by *Dey et al*., 2011) during the monsoon season facilitates the transition from low to midlevel and high clouds. Without this condition favorable for structural development of clouds, low clouds probably would have been desiccated in the presence of absorbing aerosols (as indicated by large AI values in Table 1); instead, they structurally evolve before initiation of rainfall.

[10] To better understand the role of aerosols in such structural transition, we examined the normalized anomaly of cloud vertical distribution, Δf_c (Figure 2) as function of R. f_c is dominated by low clouds when R is negative. As R transitions into positive values, low-level cloudiness reduces, as shown by the negative Δf_c, along with a corresponding increase in midlevel clouds. For example, $\Delta f_c > 0$ is observed in the altitude range 5.5–6.5 km for $0 < R < 1$, while below 4.5 km, Δf_c is negative. Positive Δf_c continues to persist (but with a smaller magnitude) above 4.5 km for $1 < R < 2$. Clouds in this altitude range are precipitated out eventually, as shown by negative Δf_c for $R > 2$ between 4.5 and 8 km altitudes. In recent CAIPEEX campaign, onset of rain in monsoon convective clouds has been observed at 6 km altitude [*Konwar et al*., 2012], similar to our results. Note that the invigoration above 4.5 km associated with the transition of Δf_c from positive to negative is atypical for the core monsoon region and is influenced by the convective strength. Continuous decrease in CTP (derived from MODIS) with an increase in R (Table 1) further supports the changes in vertical structure of monsoon clouds observed from MISR data. When classified as a function of *AOD*, CTP also shows a decrease with an increase in *AOD* at all ranges of R (Figure 3). For example, CTP reduces from ~800 hPa (~480 hPa) at $AOD < 0.3$ to ~550 hPa (~400 hPa) at $AOD > 0.7$ for $-2 < R < -1$ ($R > 2$). The magnitude of the invigoration (i.e., the reduction of CTP indicating vertical development of clouds) is ~400 hPa at $AOD < 0.3$ and continues to reduce with an increase in *AOD*. Consistent with the theoretical notion that the invigoration is favored for warm clouds [*Rosenfeld et al*., 2012; *Li et al*., 2011], largest decrease in CTP in response to a similar increase in *AOD* is observed for the lowest range of R (representing a drier condition). For example, the rate of decrease of CTP with an increase in unit *AOD* consistently reduces from 162 hPa at $-2 < R < -1$ to 77.6 hPa at $R > 2$. As the low clouds transition to midlevel and eventually high clouds due to invigoration, the sensitivity of change in CTP in response to an increasing *AOD* becomes low.

[11] The profiles of vertical wind from NCEP reanalysis data (Supporting Figure S1) reveal an increase in updraft strength between 925 and 500 hPa altitude ranges with an increase in R, which is expected in the monsoon season. Aerosols are mostly present below 500 hPa altitude over the monsoon region [e.g., *Yu et al*., 2010]. At negative R (i.e., dry condition), AI is high (1.21 ± 0.6), probably due to larger dust and smoke transport [*Ramachandran and Kedia*, 2012] and continues to decrease with an increase in R (Table 1). However, note that mean AI of 0.83 ± 0.26 even at $R > 2$ suggests that the aerosols, that were observed to be persistent throughout the monsoon season, have a large fraction of absorbing component. Aircraft measurements in the CTCZ region during the monsoon season [*Jaidevi et al*., 2011] also revealed the presence of absorbing aerosols up

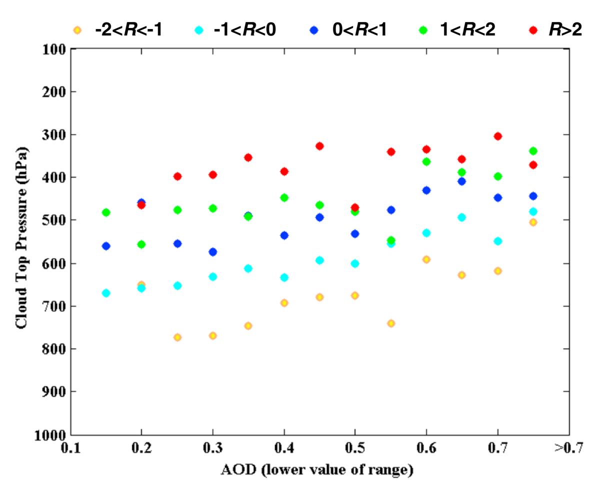

Figure 3. Variations of mean CTP **with** an increase in *AOD* as a function of R.

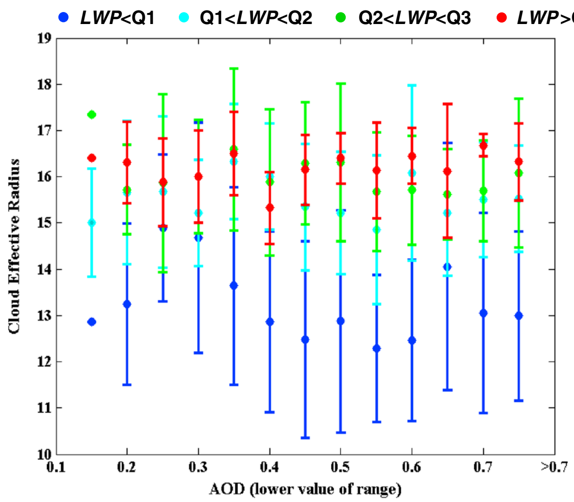

Figure 4. Variations of $R_{eff,l}$ with an increase in *AOD* as a function of *LWP*.

to 3 km altitude resulting in a large heating in the lower troposphere. In the winter season over the north Indian Ocean, the presence of absorbing aerosols led to microphysics-radiation effect [*Dey et al*., 2011]. However, such superposition is not observed here (Figure 1) for monsoon clouds because of strong updraft facilitating structural evolution of low clouds. We interpret that the presence of absorbing aerosols would certainly have local convective heating (as demonstrated in *Ramachandran and Kedia* [2012]) and that would strengthen the updraft by destabilizing the atmosphere above the aerosol layer [*Koren et al*., 2008]. At $R > 2$ (i.e., large precipitation days), strongest downdraft is seen between 300 and 450 hPa altitude ranges. To summarize the results, the aerosol dynamic effect is more of a facilitator in the invigoration of monsoon clouds rather than the main driving mechanism. In the absence of synoptic condition conducive for invigoration, low clouds probably would have desiccated in the presence of absorbing aerosols (as observed in the winter season, *Dey et al*. [2011]).

[12] To further understand the possible microphysical connection during the invigoration, we examined the relationship between *AOD* and $R_{eff,l}$ at four regimes of *LWP* (Figure 4). When available moisture is least (*LWP* < first quartile, Q1), $R_{eff,l}$ decreases with an increase in *AOD* until *AOD* reaches 0.6, beyond which the sensitivity of $R_{eff,l}$ to increasing *AOD* reduces. Aircraft measurements during CAIPEEX experiment reveal that R_{eff} must exceed the threshold of 12 µm for rainfall to be detected in the Indian monsoon region [*Konwar et al*., 2012], while other studies [e.g., *Ramachandran and Kedia*, 2012] have documented a threshold of 14 µm. It is noteworthy that $R_{eff,l}$ is larger than 14 µm at *LWP* > Q2 and it shows a random behavior in response to an increase in *AOD*. R_{eff} would have increased during the structural evolution under strong convection (as shown by high *LWP*) in the monsoon season [*Jiang et al*., 2011]. These two competing effects may cancel each other leading to this randomness in the observed relationship of *AOD*-R_{eff}. Both $R_{eff,l}$ and $R_{eff,m}$ increase with an increase in *R* (Table 1), while $R_{eff,I}$ does not show any significant change. Furthermore, $R_{eff,l}$ and *LWP* show an increase with CTH until CTH reaches ~6 km, beyond which they tend to stabilize, while the corresponding values for the ice clouds do not show any trend. Throughout, *AOD* remains high, and even shows a slight increase at CTH > 5 km, suggesting accumulation of aerosols during the invigoration by strong updraft.

4. Discussion and Conclusions

[13] The observed relationships of aerosol and cloud parameters may be influenced by remote sensing artifacts such as misclassification of clear and cloudy pixels, 3-D cloud effects, and aerosol humidification near cloud fields and hence it may be difficult to attribute the causality only to aerosols [*Koren et al*., 2010]. Here, the analysis is not restricted to *AOD* and f_c. We have also examined the vertical structure of clouds and the associated aerosol properties and cloud microphysical properties as a function of *R*. *R* shows strong correlation with the vertical development of clouds in the core monsoon region. Our results indicate that persistence of aerosols (a major fraction of which is absorbing) throughout the monsoon season may have acted as a facilitator to invigoration of clouds under favorable synoptic condition by suppressing warm rain. This has resulted in infrequent rain events, mostly when clouds are invigorated above 4.5 km altitude in the core monsoon region. Similar analysis can be carried out in other parts of the country to better understand the aerosol-monsoon connection.

[14] Our results emphasize on considering the aerosol dynamic (radiative) impacts as well as microphysical impacts to fully resolve this issue. Recent CAIPEEX campaign has provided valuable insight into aerosol-cloud microphysical relationships [e.g., *Konwar et al*., 2012; *Pandithurai et al*., 2012; *Prabha et al*., 2012], which may help in improving the existing cloud microphysical parameterization schemes of the models. Equally important to consider is the aerosol radiative feedback on the monsoon circulation at various time scales as discussed in *Ganguly et al*. [2012], particularly in view of large N-S and E-W asymmetry in aerosol loading over the Indian monsoon region reported in the literature [e.g., *Dey and Di Girolamo*, 2010]. These results will help in assessing the sensitivity studies of cloud microphysical evolution during the vertical development of convective clouds in response to aerosols using mesoscale models.

[15] The key conclusions of the present study are as follows:

[16] 1. In the last 11 monsoon seasons, the transition from negative (occurring in 84.6% days) to positive (in 15.4% days) normalized rainfall anomaly, *R* within the core monsoon region is associated with structural evolution of monsoon clouds above 4.5 km altitude. The structural evolution is further confirmed by decrease in cloud top pressure with *R*.

[17] 2. In the fully evolved monsoon clouds, droplet effective radius of warm clouds is insensitive to changes in aerosol concentration in the observed data, probably because the aerosol microphysical effect may have been nullified by meteorological effect.

[18] 3. Persistence of large aerosol loading (a fraction of which is absorbing component) within the core monsoon region acts more of a facilitator in invigorating the monsoon clouds by suppressing the warm rain, when total cloud fraction is dominated by low clouds.

[19] **Acknowledgments.** This work is supported by the Ministry of Earth Sciences, Government of India under the CTCZ program (MoES/CTCZ/16/28/10) through a research grant operational at IIT Delhi (IITD/IRD/RP2479). MISR, MODIS, and TRMM data are obtained from the

NASA Langley Atmospheric Science Data Center, while meteorological data are taken from NCEP-NCAR reanalysis. We acknowledge the comments by two anonymous reviewers who helped us improve the earlier version of the manuscript.

[20] The Editor thanks Jonathan Jiang and an anonymous reviewer for their assistance in evaluating this paper.

References

Ackerman, A. S., O. B. Toon, D. E. Stevens, A. J. Heymsfield, V. Ramanathan, and E. J. Welton (2000), Reduction of tropical cloudiness by soot, *Science*, *288*, 1042–1046.

Andreae, M. O., and D. Rosenfeld (2008), Aerosol-cloud-precipitation interactions, Part 1. The nature and sources of cloud-active aerosols, *Earth Sci. Rev.*, *89*, 13–41.

Bollasina, M. A., Y. Ming, and V. Ramaswamy (2011), Anthropogenic aerosols and the weakening of the south Asian summer monsoon, *Science*, *334*, 502–505.

Dey, S., and L. Di Girolamo (2010), A climatology of aerosol optical and microphysical properties over the Indian subcontinent from 9 years (2000–2008) of Multiangle Imaging Spectroradiometer (MISR) data, *J. Geophys. Res.*, *115*, D15204, doi:10.1029/2009JD013395.

Dey, S., L. Di Girolamo, G. Zhao, A. L. Jones, and G. McFarquhar (2011), Satellite-observed relationships between aerosol and trade-wind cumulus cloud properties over the Indian Ocean, *Geophys. Res. Lett.*, *38*, L01804, doi:10.1029/2010GL045588.

Gadgil, S. (2003), The Indian monsoon and its variability, *Annu. Rev. Earth Planet. Sci.*, *31*, 429–467.

Ganguly, D., P. J. Rasch, H. Wang, and J. Yoon (2012), Fast and slow responses of the South Asian monsoon system to anthropogenic aerosols, *Geophys. Res. Lett.*, *39*, L18804, doi:10.1029/2012GL053043.

Heymsfield, A. J., and G. M. Mcfarquhar (2001), Microphsyics of INDOEX clean and polluted trade cumulus clouds, *J. Geophys. Res.*, *D22*, 28,653–28,673.

Jaidevi, J., S. N. Tripathi, T. Gupta, B. N. Singh, V. Gopalakrishnan, and S. Dey (2011), Observation-based 3-D view of aerosol radiative properties over Indian Continental Tropical Convergence Zone: Implications to regional climate, *Tellus*, *63B*, 971–989.

Jiang, J. H., H. Su, C. Zhai, S. T. Massie, M. R. Schoeberl, P. R. Colarco, S. Platnick, Y. Gu, and K.-N. Liou (2011), Influence of convection and aerosol pollution on ice cloud particle effective radius, *Atmos. Chem. Phys.*, *11*, 457–463.

Kahn, R. A., D. Nelson, M. Garay, R. Levy, M. Bull, D. Diner, J. Martonchik, S. Paradise, E. Hansen, and L. Remer (2009), MISR aerosol product attributes and statistical comparisons with MODIS, *IEEE Trans. Geosci. Remote Sens.*, *47*(12), 4095–4114.

Konwar, M., R. S. Maheshkumar, J. R. Kulkarni, E. Freud, B. N. Goswami, and D. Rosenfeld (2012), Aerosol control on depth of warm rain in convective clouds, *J. Geophys. Res.*, *117*, D13204, doi:10.1029/2012JD017585.

Koren, I., J. Vanderlei Martins, L. A. Remer, and H. Afargan (2008), Smoke invigoration versus inhibition of clouds over the Amazon, *Science*, *321*, 946–949.

Koren, I., G. Feingold, and L. A. Remer (2010), The invigoration of deep convective clouds over the Atlantic: Aerosol effect. Meteorology or retrieval artifact?, *Atmos. Chem. Phys.*, *10*, 8855–8872.

Lau, K. M., and K. M. Kim (2006), Observational relationships between aerosol and Asian monsoon rainfall and circulation, *Geophys. Res. Lett.*, *33*, L21810, doi:10.1029/2006GL027546.

Levy, R. C., L. A. Remer, R. G. Kleidman, S. Mattoo, C. Ichoku, R. Kahn, and T. F. Eck (2010), Global evaluation of the Collection 5 MODIS dark-target aerosol products over land, *Atmos. Chem. Phys.*, *10*, 10,399–10,420, doi:10.5194/acp-10-10399-2010.

Li, Z., F. Niu, J. Fan, Y. Liu, D. Rosenfeld, and Y. Dang (2011), Long-term impacts of aerosols on the vertical development of clouds and precipitation, *Nat. Geosci.*, *4*, 888–894.

Marchand, R., T. Ackerman, M. Smyth, and W. B. Rossow (2010), A review of cloud top height and optical depth histograms from MISR, ISCCP, and MODIS, *Geophys. Res. Lett.*, *115*, doi:10.1029/2009JD013422.

Min, Q., E. Joseph, Y. Lin, L. Min, B. Yin, P. H. Daum, L. I. Kleinman, J. Wang, and Y.-N. Lee (2012), Comparison of MODIS cloud microphysical properties with in-situ measurements over the Southeast Pacific, *Atmos. Chem. Phys.*, *12*, 11,261–11,273, doi:10.5194/acp-12-11261-2012.

Pandithurai, G., S. Dipu, T. V. Prabha, R. S. Maheskumar, J. R. Kulkarni, and B. N. Goswami (2012), Aerosol effect o droplet spectral dispersion in warm continental cumuli, *J. Geophys. Res.*, *117*, D16202, doi:10.1029/2011JD016532.

Prabha, T. V., S. Patade, G. Pandithurai, A. Khain, D. Axisa, P. Pradeep-Kumar, R. S. Maheshkumar, J. R. Kulkarni, and B. N. Goswami (2012), Spectral width of premonsoon and monsoon clouds over Indo-Gangetic valley, *J. Geophys. Res.*, *117*, D20205, doi:10.1029/2011JD016837.

Prasad, A. A., and R. Davies (2012), Detecting tropical thin cirrus using Multiangle Imaging SpectroRadiometer's oblique cameras and modeled outgoing longwave radiation, *J. Geophys. Res.*, *117*(D6), D06208, doi:10.1029/2011JD016798.

Ramachandran, S., and S. Kedia (2012), Aerosol, clouds and rainfall: inter-annual and regional variations over India, *Clim. Dyn.*, *40*(7–8), 1591–1610.

Ramanathan, V., C. Chung, D. Kim, T. Bettge, L. Buja, J. T. Kiehl, W. M. Washington, Q. Fu, D. R. Sikka, and M. Wild (2005), Atmospheric Brown Clouds: Impacts on South Asian Climate and Hydrological Cycle, *Proc. Natl. Acad. Sci.*, *102*, 5326–5333.

Rosenfeld, D., H. Wang, and P. J. Rasch (2012), The roles of cloud drop effective radius and LWP in determining rain properties in marine stratocumulus, *Geophys. Res. Lett.*, *39*, L13801, doi:10.1029/2012GL052028.

Small, J. D., J. H. Jiang, H. Su, and C. Zhai (2011), Relationship between aerosol and cloud fraction over Australia, *Geophys. Res. Lett.*, *38*, L23802, doi:10.1029/2011GL049404.

Stubenrauch, C. J., et al. (2013), Assessment of global cloud datasets from satellites: Project and database initiated by the GEWEX radiation panel, *Bull. Am. Meteorol. Soc.*, *94*, 1031–1049.

Tao, W.-K., J.-P. Chen, Z. Li, C. Wang, and C. Zhang (2012). Impact of aerosols on convective clouds and precipitation, *Rev. Geophys.*, *50*, RG2001, doi:10.1029/2011RG000369.

Torres, O., A. Tanskanen, B. Veihelmann, C. Ahn, R. Braak, P. K. Bhartia, P. Veefkind, and P. Levelt (2007), Aerosols and surface UV products from ozone monitoring instrument observations: An overview, *J. Geophys. Res.*, *112*, D24S47, doi:10.1029/2007JD008809.

Wu, D. L., et al. (2009), Vertical distributions and relationships of cloud occurrence frequency as observed by MISR, AIRS, MODIS, OMI, CALIPSO and CloudSat, *Geophys. Res. Lett.*, *36*, L09821, doi:10.1029/2009GL037464.

Yu, H., M. CHin, D. M. Winker, A. L. Omar, Z. Liu, C. Kittaka, and T. Diehl (2010), Global view of aerosol vertical distributions from CALIPSO lidar measuremnets and GOCART simulations: Regional and seasonal variations, *J. Geophys. Res.*, *115*, D00H30, doi:10.1029/2009JD013364.